The apoptotic and anti-proliferative effect of Lysyl oxidase propeptide in Y79 human retinoblastoma cells

Nareshkumar Ragavachetty Nagaraj,[1,2] Sulochana Konerirajapuram Natarajan,[1] Coral Karunakaran[1]

Retinoblastoma (RB) is a primary ocular malignancy affects only one eye (unilateral) unlike the germline mutation

[1]*RS Mehta Jain Department of Biochemistry and Cell biology, KBIRVO, Vision Research Foundation, Chennai;* [2]*School of Chemical and Biotechnology, SASTRA Deemed to be University, Thanjavur, India*

Purpose: Retinoblastoma (RB) caused by the mutation of the *RB1* gene is one of the most common ocular malignancies in children The propeptide region of lysyl oxidase (LOX), the enzyme involved in the cross-linking of collagen and elastin, has been identified to be anti-tumorigenic in various cancers. However, this role of lysyl oxidase propeptide (LOX-PP) in RB is still elusive. This study aims to identify the anti-tumorigenic effect of LOX-PP in human Y79 RB cells.
Methods: LOX-PP was overexpressed in Y79 RB cells, and differential gene expression was assessed by microarray followed by pathway analysis using transcriptome analysis console (TAC) software. Additionally, cell proliferation was studied by PrestoBlue assay, and DNA content was evaluated by cell cycle and apoptosis assays. The pro-apoptotic and anti-proliferative mechanisms induced by the overexpression of/exogenously added LOX-PP was evaluated by western blotting and real-time PCR.
Results: The expression of the *LOX-PP* transcript was significantly decreased in Y79 RB cells compared to human retinal endothelial cells. Gene expression analysis in LOX-PP overexpressed Y79 RB cells showed deregulation of pathways involved in apoptosis, cell cycle, focal adhesion-PI3K-AKT signaling, and DNA repair mechanisms. Interestingly, LOX-PP overexpressed Y79 RB cells showed significantly increased apoptosis, decreased proliferation, and cell cycle arrest at S-phase with a concordant reduction of proliferative cell nuclear antigen and Cyclin D1 protein expressions. Moreover, pAKT (S473) was significantly downregulated in Y79 RB cells, which decreased NFκB leading to significantly reduced BCL2 expression.
Conclusions: Our results demonstrate the anti-tumorigenic effect of LOX-PP in Y79 RB cells by inducing apoptosis and decreasing proliferation. This effect was mediated by the downregulation of AKT signaling. These results suggest that LOX-PP can be explored as a therapeutic molecule in RB.

with about 1500 new cases diagnosed in India every year in children below five years of age [1]. It is caused by a biallelic mutation in the *RB1* gene. In 1971, Knudson proposed the "two-hit" hypothesis, which states that the development of RB requires two chromosomal mutations. The first hit occurs as a germline mutation, which is inherited and found in all the cells, while the second hit develops only in somatic retinal cells [2]. The loss of both alleles of the *RB1* [3] tumor-suppressor gene leads to uncontrolled retinal progenitor cell proliferation due to the over-activation of E2F, thereby preventing cell-cycle exit [4]. The occurrence of RB can either be bilateral or unilateral. *RB1* germline mutation accounts for 40% of all RB cases, exhibiting its autosomal dominant inheritance. Further, in 60% of the sporadic form, it

(bilateral) [5].

RB, if diagnosed early, can be effectively treated; however, in advanced cases, it spreads along the optic nerve and invades the brain due to its metastatic properties [6]. The incidence of metastasis increases based on various clinical risk factors that include the patient's age, vascularity, laterality, and the stage of diagnosis [7]. The therapies currently available for RB are non-specific and thus fail to accomplish complete remission [8]. External beam radiotherapy, although highly effective in many RB tumors, possesses a high risk of second primary cancers [9]; therefore, it has been replaced with systemic chemotherapy. Chemotherapy is usually administered as a combination of etoposide, carboplatin, and vincristine. It can be combined with cryotherapy and focal laser treatment, which provides improved efficiency and reduces the incidence of enucleation. Nevertheless, chemotherapy holds disadvantages such as bone marrow suppression, infections, and the possibility of developing

Correspondence to: K. Coral Miriam, R. S.Mehta Jain Department of Biochemistry and Cell Biology, KBRIVO, Vision Research Foundation, 41, College Road, Chennai-600006, India. email: ceeyem08@gmail.com

secondary cancers such as leukemia [8]. To overcome these issues, several groups are working on identifying new drugs and/or adjuvant therapies. Liu et al. established a RB organoid model derived from genetically engineered human embryonic stem cells to test the novel therapeutic agents for human RB [10]. Recently, Ping Li et al. established a RB organoid model from patient-induced pluripotent stem cells with the straightforward evidence of the Knudson two-hit hypothesis as a promising alternative, in vivo RB model to test candidate therapeutic molecules [11].

Lysyl oxidase (LOX; protein −6-oxidase) is an amine oxidase enzyme required for the cross-linking of collagen and elastin [12,13]. LOX is secreted as an immature precursor (50 kDa), which is then cleaved by bone morphogenetic protein −1 (BMP1) into a C-terminal active mature enzyme (LOX; 32 kDa) and an N-terminal lysyl oxidase propeptide (LOX-PP; 18 kDa) [14-17]. Contente et al. and Kenyon et al. identified that *LOX* acts as the "*ras recision gene*" [18,19]. Prostate, colorectal, lung, and breast cancer-derived cell lines show reduced LOX expression [20]. LOX enzyme activity is considered to possess tumor-inhibiting properties, and a decreased enzymatic activation of LOX was observed in several cancerous cell lines compared with non-cancerous cell lines [20]. However, when the activity of LOX is inhibited by its classic inhibitor β-aminopropionitrile, it fails to re-transform the phenotypic reversion of *ras*-transformed fibroblast. *LOX* gene silencing experiments increased phenotypic reversion and induced tumorigenesis, thus indicating that the tumor-suppressor property is not dependent on LOX activity but its transcript expression. Further, it was identified that the anti-tumorigenic activity of the propeptide region of LOX is involved in the inhibition of *ras*-transformed phenotype and *ras*-mediated signaling in fibroblasts [21] and Her-2/neu-driven NF639 breast cancer cells [22]. However, so far there have been no reports on the role of LOX-PP in ocular tumors such as RB. Here, we report that the basal levels of LOX-PP are reduced in Y79 RB cells. The overexpression of LOX-PP/addition of recombinant LOX-PP (rLOX-PP) decreased Y79 cell proliferation, increased apoptosis, and reduced the expression of proliferative cell nuclear antigen (PCNA) and Cyclin D1, through the downregulation of AKT-mediated NFκB activity, further inhibiting BCL-2. Thus, our data are the first to report an apoptotic and anti-proliferative role of LOX-PP in Y79 RB cells.

METHODS

Ethics statement: The Ethics Sub-Committee and the Institutional Review Board of Vision Research Foundation, Chennai, India, approved all experiments using human donor eyeball (Approval No: 140–2008-P, dated: 26.03.2009 and Approval No: 357–2012-P, dated: 21.02.2013). The experiments were conducted according to the tenets of the Declaration of Helsinki.

Cell culture: Y79 RB cells (NCCS, India) and NCC-RBC51 (kind gift from Dr. S. Krishnakumar, Department of Ocular Pathology, Vision Research Foundation) were cultured in RPMI 1640 medium (Hyclone, UK) with 10% fetal bovine serum (Gibco) and antibiotic–antimycotic (Gibco) solution in 5% CO_2 at 37 °C. Human retinal endothelial cells (hRECs) were isolated from a human donor eyeball [23] and was maintained in EGM-2 medium (Lonza, Switzerland) at 5% CO_2. The Y79 cell line was authenticated with short tandem repeats (STR) analysis. The STR results showed that the DNA of the cell line perfectly matched Y79, and no cross contamination of human cells was detected (Appendix 1).

RNA isolation and cDNA synthesis: Total RNA was extracted from 2×10^6 cells using TriZol reagent (Sigma Aldrich). The RNA was further treated with DNase (NEB). Total RNA was quantified in the Nanodrop spectrophotometer (Thermo Scientific). Further, 1 µg of the total RNA was converted to cDNA (cDNA) using the iScript cDNA conversion kit (Biorad).

Quantitative PCR: LOX-PP transcripts were amplified using the primers listed in Table 1. The endogenous *LOX* and *LOX-PP* transcripts were quantified by quantitative real-time PCR (CFX96, Biorad) in Y79 and NCC-RBC51 cell line. The data were analyzed based on the $2^{-\Delta\Delta ct}$ method after normalizing with the housekeeping gene, *18S rRNA* [24].

Cloning of LOX-PP in Y79 RB cells: The human LOX-PP was amplified along with the signal peptide from HUVEC cDNA using the primers listed in Table 1. The amplified LOX-PP cDNA with signal peptide was cloned in-frame into the *BamHI* and *Hind*III sites of the mammalian expression vector pcDNA3.1(+)/His A (Invitrogen). The construct was sequenced for confirmation using ABI 3100–Avant Genetic analyzer (Applied Biosystems) [25].

Overexpression in Y79 RB cells: Y79 cells were cultured in 6 well dishes at a cell density of 2×10^5 per well in RPMI 1640 medium containing 1% fetal bovine serum (FBS; no antibiotic). Transfection complex containing 2 µg of LOX-PP clone and 4 µl of X-tremeGENE HP DNA transfection reagent (Roche, Canada) was added into 200 µl of plain RPMI 1640 medium per well. It was incubated for 15 min at room temperature. The transfection complex was then added drop-wise into the 6-well plate containing Y79 cells. It was mixed gently and incubated in 5% CO_2 incubator for 4 h at 37 °C. Next, we added 1 ml of RPMI 1640 medium containing 20% FBS

without removing the transfection mixture and incubated the cells for 24, 48, 72, and 96 h. As a control, we used an empty vector (EV). After incubation, the overexpression of LOX-PP was examined at the mRNA and protein levels.

Microarray – Sample preparation and data analysis: Total RNA was extracted from 2×10^6 LOX-PP-transfected and EV-transfected Y79 cells using Trizol reagent, treated with DNase I (NEB) and quantified using Nanodrop spectro-photometer (Thermo Scientific). RNA samples were then subjected to amplification and biotinylation, and hybridized using Affymetrix HTA2.0 arrays (Thermo Scientific). These arrays were scanned with an Affymetrix gene chip 3000 fluorescent scanner. Image generation and feature extraction were performed using Affymetrix gene chip command console software. The raw data were analyzed using TAC 2.0 software, which allows for the identification of differentially expressed genes in the sample. We performed an unpaired Student *t* test to compare gene intensities between LOX-PP-transfected versus EV-transfected cells. Genes were considered significantly deregulated with a fold change, linear < -1.5 or $> +1.5$. The study was conducted in biologic duplicates (Transcriptome Analysis Console (TAC) 4.0 User Guide)

Validation of microarray data by quantitative PCR: Total RNA was extracted from 2×10^6 LOX-PP-transfected and EV-transfected Y79 cells. One μg of RNA was converted to cDNA using the iScript cDNA conversion kit (Biorad). Real-time PCR for TP53, MDM2, and BCL2 was performed, and the primers used are given in Table 1. The data were analyzed using the $2^{-\Delta\Delta ct}$ method after normalizing with *18S rRNA* [24].

Proliferation assay: For proliferation assay, 5×10^3 Y79 RB cells were transiently transfected with 0.1 μg of LOX-PP clone and EV expression plasmids and were then cultured

in 96 well dishes for 24 h. After 24 h of transfection, 10 μl of PrestoBlue (Thermo Fisher Scientific) was added to the wells. Further, the cells were incubated at 37 °C in a 5% CO_2 incubator for 24 h. The fluorescence was quantified using SpectraMax M2e (Molecular Devices) at an emission wavelength of 615 nm and an excitation wavelength of 535 nm. The intensity of the color formation is directly proportional to cell proliferation.

Apoptosis assay: For apoptosis assay, cell death ELISA, which quantifies the extent of mono and oligonucleosomes produced in the cytoplasm of lysed cells, was used. Y79 cells were cultured in 12 well dishes at a cell density of 5×10^4 cells per well in 0.4 ml of RPMI 1640 medium consisting of 1% FBS. Cells were transiently transfected with 1 μg of LOX-PP clone and EV construct, then after 4 h, 0.5 ml of RPMI 1640 medium with 20% FBS was added and incubated further for 48 h. After centrifugation at $1500 \times g$ for 5 min, the cell pellet was lysed with an incubation buffer at 25 °C for 30 min and centrifuged at $20,000 \times g$ for 10 min at 4 °C to remove nuclear debris. Then 400 μl of the supernatant was carefully separated and tested by cell death ELISA as per the manufacturer's instructions (Roche, Canada) and measured using SpectraMax M2e (Molecular Devices). For DAPI staining, the cells were fixed with 4% paraformaldehyde for 10 min and stained with DAPI for 3 min. Then the slides were observed under Axio vision fluorescence microscopy.

Cell cycle analysis: Y79 RB cells were seeded in 6 wells at a density of 2×10^5 cells per well of RPMI 1640 medium with 1% FBS. They were transiently transfected with 2 μg of LOX-PP construct and EV plasmid, then after 4 h, 1 ml of RPMI 1640 medium with 20% FBS was added and was further incubated for 48 h. After incubation, cells were permeabilized for 30

S.No	Gene name	Primers
		TABLE 1. PRIMERS LISTS AND IT SEQUENCES.

S.No	Gene name	Primers
1	LOX-PP cloning primers	FP - 5′GTTTAAACTTAAGCTTATGCGCTTCGCCTGGACC 3′
		RP - 5′CCACCACACTGGATCCCTAGCCCACCATGCCGTC 3′
2	LOX-PP	FP –5′AGCGGTGACTCCAGATGAGC 3′
		RP –5′GGCTCACAGTACCAGCCTCA 3′
3	BCL2	FP – 5′ATTTGGCAGGGGCAGAAAAC 3′
		RP –5′GCTGTGGAGAGAATGTTGGC 3′
4	TP53	FP –5′ACCTATGGAAACTACTTCCTG 3′
		RP –5′ACCATTGTTCAATATCGTCC 3′
5	MDM2	FP –5′CCTTAGCTGACTATTGGAAATG 3′
		RP –5′TGTTGAGTTTTCCAGTTTGG 3′
6	18S rRNA	FP –5′AAACCGTTGAACCCCATT 3′
		RP –5′CCATCCAATCGGTAGTAG 3′

min with 30% ethanol. Then the cells were washed with cold phosphate buffered saline (PBS; NaCl 8 g, KCl 0.2 g, Na_2HPO_4 1.4 g KH_2PO_4 0.2 g) twice and treated for 20 min with RNase (1 mg/ml). Further, the cells were incubated for 30 min with propidium iodide, and cell cycle analysis was done using FACS Calibur (Beckman Dickinson).

Western blot: 2.5×10^6 Y79 RB cells were transfected/added with recombinant LOX-PP (rLOX-PP) for 48 h. The recombinant LOX-PP was generated in our laboratory earlier and was used in this study to understand its role in Y79 RB cells [25]. rLOX-PP exposed cells were treated with 1 µM wortmannin (Cell Signaling Technology, USA) for 24 h. After incubation, cells were lysed and protein was extracted in a radioimmunoprecipitation assay lysis buffer containing 0.15 M sodium chloride, 0.5% sodium deoxycholate, 0.1% TritonX-100, 50 mM Tris with pH 8.0, and 0.1% sodium dodecyl sulfate (SDS) with phosphatase and protease inhibitor cocktail (Cell Signaling Technology). Protein quantification was performed by the BCA method (Pierce). Protein concentration containing 50 µg was separated by SDS-Poly acrylamide gel electrophoresis and transferred to polyvinylidene fluoride membrane (GE Healthcare, USA). Overnight incubation was done with LOX-PP (in-house), human AKT, human phospho AKT, human NFκB, human BCL2, human Cyclin D1, human PCNA (1 in 1000, Cell Signaling Technology), human β – actin (1 in 2000, Santa Cruz Biotechnology, Santa Cruz, CA) primary antibodies at 4 °C after blocking the membrane in Tris buffered saline with tween (TBST; 1x) containing 5% BSA for 1 h. Immunoprecipitation of LOX-PP was performed to measure the secretary LOX-PP in the overexpressed condition medium [25]. Following incubation with primary antibodies, the membranes were washed with 1X TBST thrice. Then the membranes were incubated with horseradish peroxidase conjugated secondary antibodies, respectively, for 2 h. The membranes were then washed with TBST thrice and developed using ECL plus chemiluminescence reagent (GE Healthcare), and the images were photographed using FluorChem FC3 (Protein Simple) followed by quantification using the NIH ImageJ analysis software (NIH).

Statistical analysis: All experiments were performed in triplicates independently unless otherwise mentioned. The data were expressed as mean ± SD. Student *t* test and one-way ANOVA analysis were conducted to calculate the significance. A p value of <0.05 was considered to be statistically significant.

RESULTS

Reduced expression of LOX-PP transcript in Y79 and NCCRBC51 cells: RNA from both Y79 and NCC RBC51 cells were evaluated for the presence of the *LOX-PP* transcript. The Y79 (Figure 1A) and NCC-RBC51 (Appendix 2) cells showed ~10 fold decreased expression of *LOX-PP* transcripts when compared with hRECs through real-time PCR. Earlier studies have used hRECs as a control to compare relative gene expression in RB cells [26]. Our data thus indicate that the inherent LOX-PP expression is decreased in Y79 and NCC RBC51 cells, thus evoking much interest to overexpress the LOX-PP and understand its functional relevance. As both the cell lines showed decreased expression LOX-PP, we further studied the effect of LOX-PP overexpression in Y79 cells, which are widely used for studying RB. Hence, we evaluated
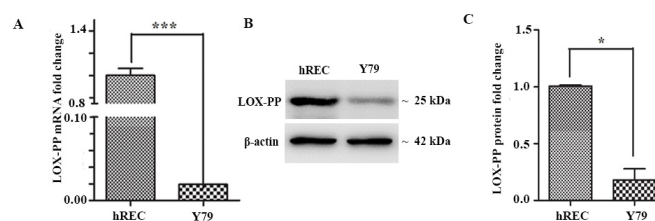

Figure 1. Expression of *LOX-PP* in Y79 RB cells and hREC primary cells. **A:** The bar diagram represents the expression of LOX-PP in fold change relative to hRECs with a p value of 0.001. **B:** Western blot analysis showing LOX-PP protein expression; it was normalized with β-actin. **C:** The bar diagram represents the quantification of LOX-PP expression in Y79 and hRECs with a p value of 0.001. Values were expressed as mean ± SD, n=3. (***p<0.001, **p<0.01, and *p<0.05, when compared with hRECs) (hRECs, human retinal endothelial cells; RB, retinoblastoma).
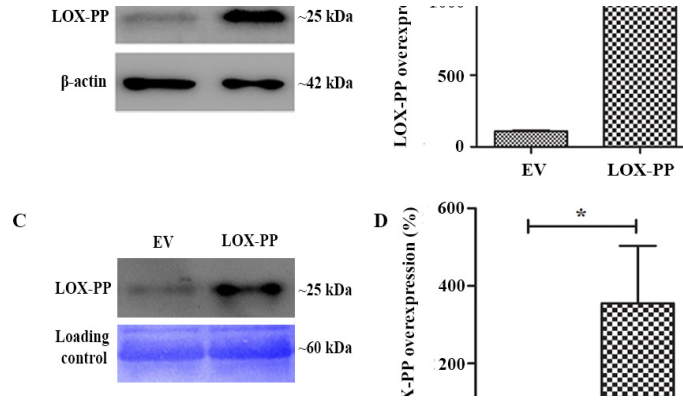
Figure 2. LOX-PP overexpression in Y79 cells. **A:** Western blot analysis showing the overexpression of LOX-PP in cell extract normalized with a housekeeping gene, β-actin. **B:** The bar diagram represents LOX-PP overexpression in cell extracts compared to EV in percentage, with a p value of less than 0.01. **C:** Western blot analysis showing the expression of secretary extracellular LOX-PP normalized with a loading control. **D:** The bar diagram represents LOX-PP overexpression in conditioned medium compared to EV in percentage with a p value of 0.042. Values were expressed as mean ± SD, n=3. (Student *t* test was used for statistical analysis; ***p<0.001, **p<0.01, and *p<0.05, when compared with EV) (EV, empty vector).

the LOX-PP protein expression in Y79 cells and found it to be decreased (Figure 1B, C).

The overexpression of LOX-PP in Y79 cells: LOX-PP with the signal peptide was cloned and overexpressed in a mammalian expression construct in Y79 cells (pcDNA 3.1/ His A + LOX-PP). The overexpression of LOX-PP in Y79 cells was confirmed at the transcript and translational levels by quantitative PCR and western blotting, respectively. The

highest expression was seen 48 h post transfection at transcript levels (Appendix 3) when compared with other time points. The N-glycosylated form of LOX-PP (~25 kDa) was observed in cell extracts subjected to western blot analysis (Figure 2A). An efficient expression of ~50 fold was found in LOX-PP overexpressed cells compared to EV with a significant p value of <0.01 (Figure 2B). The immunoprecipitation of extracellular LOX-PP overexpressed condition medium showed a significant (Figure 2C, D) increase in the
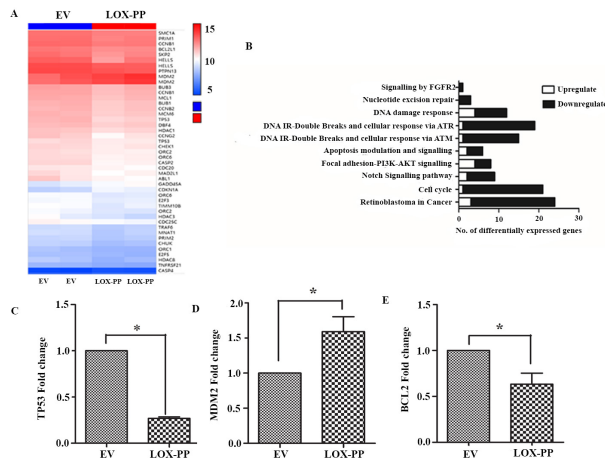

Figure 3. Microarray analyses in Y79 cells overexpressed with LOX-PP. **A:** Heatmap of differentially expressed genes in LOX-PP overexpressed Y79 cells. **B:** List of pathways deregulated upon LOX-PP overexpression. **C:** Microarray data validation by quantitative PCR for TP53 (p<0.05), **D:** BCL2 (p<0.05), and **E:** MDM2 (p<0.05). Values were expressed as mean ± SD, n=3. (Student *t* test was used for statistical analysis; ***p<0.001, **p<0.01, and *p<0.05, when compared with EV) (EV, empty vector).

TABLE 2. LIST OF PATHWAYS DEREGULATED UPON LOX-PP OVEREXPRESSION IN Y79 RETINOBLASTOMA CELLS.

Pathway name	Upregulated genes	Downregulated genes	p value
Retinoblastoma (RB) in Cancer	MDM2,CDKN1A,MIR29B1	HDAC1,SKP2,TP53,PLK4,CCNB1CCNB2,MCM6,RFC5,POLA1,PRIM1,ORC1,CHEK1,TTK,SMC2,KIF4A,HMGB1,SMC1A,FAF1,POLD3,RBBP4,E2F3	0
Cell Cycle	MDM2	ATR,BUB1,BUB3,HDAC1,HDAC8,CCNB1,CCNB2,SKP2,SMC1A,E2F3,E2F5,CDC20,APC,YWHAG,YWHAB,MCM6,MCM8,ORC1,ORC2,ORC6	0.000032
Notch Signaling Pathway	CDKN1A,HES1	MAML2,APH1A,NCSTN,MAML3,HDAC1,NUMB,JAK2	0.048418
Focal Adhesion-PI3K-Akt-mTOR-signaling pathway	ITGB5,IL2,MDM2,CDKN1A	JAK2,IGF1R,KRAS,RAB10	0.000412
Apoptosis Modulation and Signaling	MIR29B1,CASP4	CASP2,TRAF6,TP53,MCL1	0.023205
DNA IR-Double Strand Breaks (DSBs) and cellular response via ATM	MDM2	ATR,EXO1,MRE11A,ACTL6A,TP53,DCLRE1C,TRAF6,BLM,BRCA2,SMC1A,LATS1,BRCA1,RNF8,RIF1	0.000021
DNA IR-damage and cellular response via ATR	MDM2	ATR,FANCI,MRE11A,TP53,SMC1A,BLM,XRCC5,BRCA2,EXO1,EEF1E1,TDP1,BRCA1,RNF8,TOPBP1,BRIP1,HUS1,WRN,FOXM1	0.000147
DNA Damage Response	GADD45A,CDKN1A,DDB2,MDM2	ATR,SMC1A,CCNB1,CHEK1,TP53,BRCA1,HUS1,CCNB2	0.004928
Nucleotide Excision Repair		CHD1L,TCEA1,RNF111	0.002604
Signaling by FGFR2		BRAF	0.000011

expression of N-glycosylated LOX-PP (>25 kDa). No cell toxicity was observed by the 3-(4,5-dimethylthiazol-2-yl)-2,5-diphenyltetrazolium bromide (MTT) assay (data not shown) and hence 48 h were fixed as a time point for the subsequent experiments.

Effect of LOX-PP on differential gene expression: Differential gene expression profiles of LOX-PP-transfected and EV-transfected cells were performed using HTA2.0 GeneChip Arrays (Affymetrix®) that contain 70,523 detectable transcripts using TAC 4.0 software. The analysis showed that 212 genes were differentially expressed, with 69 genes upregulated and 143 genes downregulated in LOX-PP-transfected cells when compared to EV. The heat map represents the fold change of gene expression, where downregulated genes are in blue and upregulated genes are in red color (Figure 3A). This data are available for download at the gene expression omnibus (GEO) database accession (GSE119413). These genes were annotated using gene ontology for categorizing based on the molecular function and a biologic process. Figure 3B lists the major signaling pathways deregulated upon LOX-PP

overexpression in Y79 cells, namely RB in cancer, focal adhesion-PI3K-AKT signaling cell cycle, apoptosis, FGFR2, and DNA repair mechanisms. As revealed by the pathway analysis in Table 2, the majority of the deregulated genes are involved in DNA replication (*E2F3, KIF4A, HMG2, HDAC1*), cell cycle progression (*CCNB2, CDKN1A*), and apoptosis (*BCL2L1, MCL1*), as shown in Figure 4.

Further, the deregulated genes, *TP53, MDM2,* and *BCL2,* from the microarray profile were validated by real-time PCR. TP53 (Figure 3C) and BCL2 (Figure 3D) were significantly decreased, *MDM2* (Figure 3E) was significantly increased in LOX-PP overexpressed Y79 RB cells. Since LOX-PP overexpressed Y79 cells showed deregulation in apoptosis, DNA replication, and cell cycle progression pathway, we further performed in vitro functional assays such as proliferation, apoptosis, and cell cycle to confirm the microarray analysis.

LOX-PP decreases cell proliferation in Y79 cells: RB tumors are highly angiogenic [7], and the critical event in angiogenesis is proliferation. Y79 RB cells that were transfected with LOX-PP showed significantly decreased cell proliferation
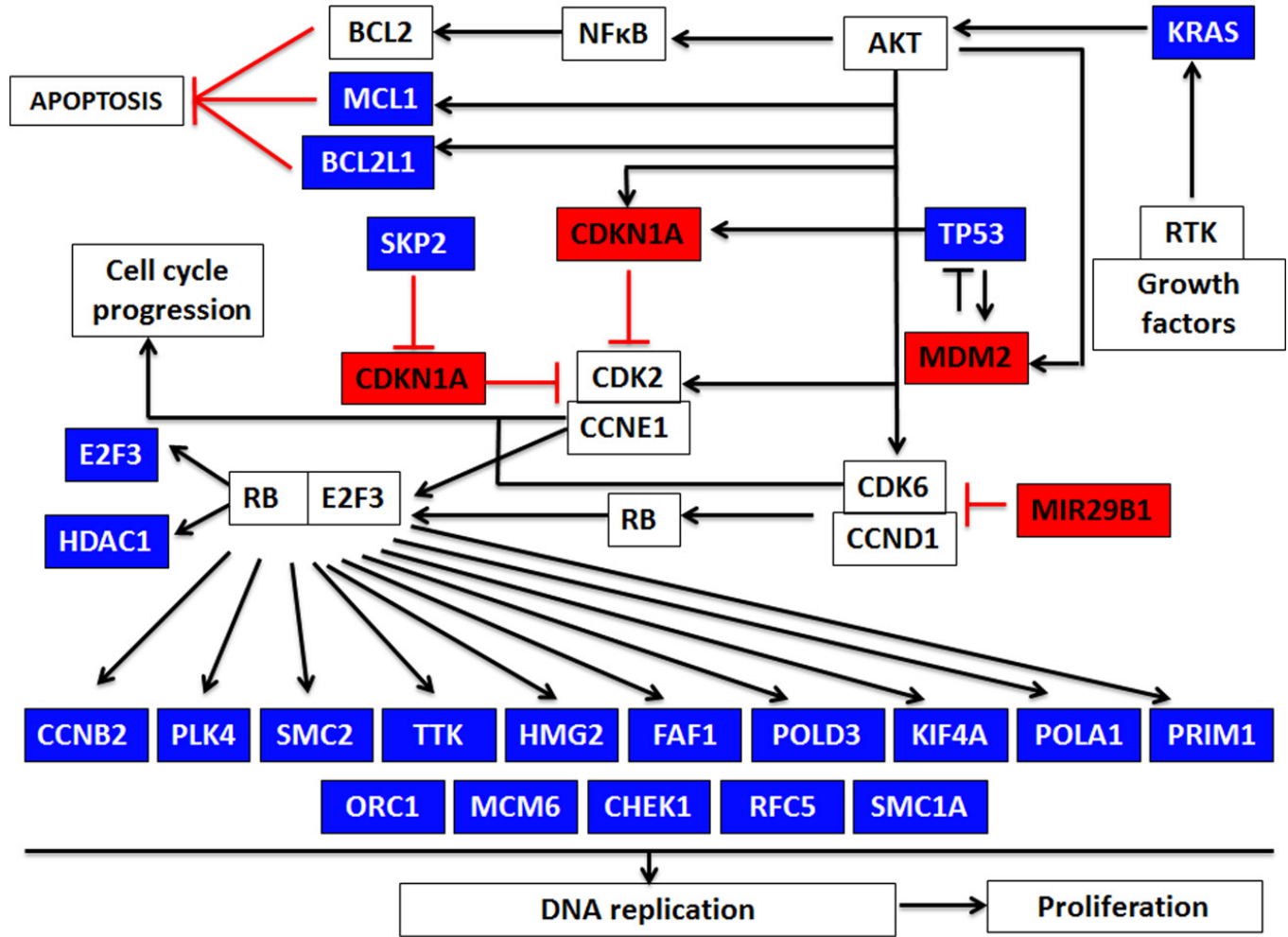
Figure 4. Pathway analysis on microarray data of Y79 RB cells upon LOX-PP overexpression. Representation of RB, cell cycle, and PI3K-AKT-Focal adhesion pathway highlighting gene regulation upon LOX-PP overexpression. Red indicates upregulation of genes with the overexpression of LOX-PP, while green indicates downregulation compared to empty vector. (RB, retinoblastoma).

(p<0.001) compared with EV (Figure 5A). Besides, to investigate the antiproliferative mechanism of LOX-PP, we evaluated the effect of LOX-PP on the expression of the proliferative marker, PCNA. Interestingly, PCNA expression was significantly decreased in LOX-PP overexpressed Y79 RB cells compared with EV (Figure 5B, C). This was further confirmed by the addition of 2.5 µg/mL of recombinant LOX-PP (rLOX-PP) to Y79 RB cells, which showed a similar inhibition of PCNA (Figure 5D,E; p<0.01), thereby highlighting the proliferation inhibitory role of LOX-PP in Y79 RB cells.

LOX-PP induces apoptosis in Y79 cells: Tumor suppressors exert their anti-tumorigenic potential by inducing apoptosis [27]. Y79 RB cells that were overexpressed with LOX-PP showed significantly increased apoptosis (p<0.05) when compared with EV at 48 h (Figure 6A). This was also further

confirmed with apoptotic morphological detection through DAPI staining. Further, 2.5 µg/mL of rLOX-PP treated cells showed increased apoptosis compared to vehicle control (Figure 6B). This validated our findings in microarray analyses (Figure 3B), where LOX-PP overexpression downregulated BCL-2 involved in the anti-apoptotic event. To further confirm this effect, the cell cycle analysis was conducted at the same time point.

LOX-PP arrested cells in S-phase: We examined the effect of LOX-PP overexpression in the cell cycle. LOX-PP overexpression significantly arrested cells in the S phase (p<0.01) and reduced cells in the G0-G1 phase at 48 h (Figure 7A, B). To strengthen the observation, we assessed the Cyclin D1 expression, which is a cell cycle checkpoint. Y79 RB cells overexpressing LOX-PP showed significantly reduced Cyclin D1 expression compared to EV (Figure 7C, D). Similar results
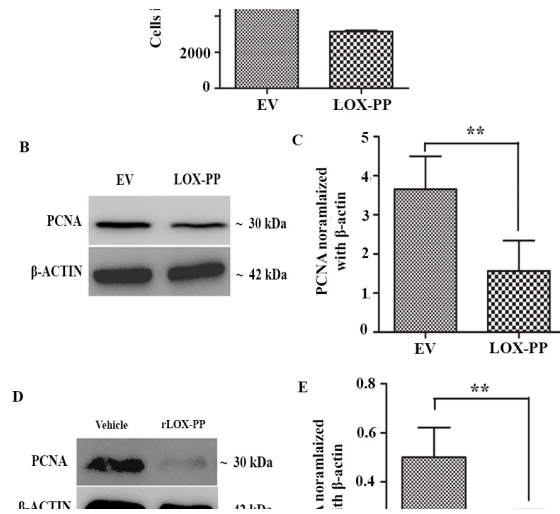
Figure 5. Y79 cell proliferation influenced by LOX-PP. **A:** Quantification of the results of the proliferation assay. **B:** Western blot analysis showing the expression of PCNA in Y79 cells were overexpressed with LOX-PP. **C:** The bar diagram shows the quantification of PCNA normalized with β-actin. **D:** Western blot for PCNA upon addition of 2.5μg/ml of rLOX-PP in Y79 retinoblastoma cells. **E:** The bar diagram represents the quantification of PCNA normalized with β-actin. Values were expressed as mean ± SD, n=3. (Student *t* test statistical analysis was used; ***p<0.001, **p<0.01, and *p<0.05, when compared with EV and vehicle control) (EV, empty vector)

were observed upon the addition of rLOX-PP (Figure 7E, F). These findings correlate with our microarray results where the LOX-PP overexpressed Y79 RB cells showed *CCNB1, CCNB2, HDAC1,* and *E2F3* genes involved in the cell cycle to be downregulated.

Effect of LOX-PP on pAKT, NFκB, and BCL-2 in Y79 cells: The proliferation of Y79 cells was reduced, and apoptosis was increased in LOX-PP overexpressed cells. Apoptosis can also be regulated by AKT and its constitutive activation of NFκB, which is a downstream effector of AKT. We studied the effect of LOX-PP in AKT-NFκB signaling. Figure 8A shows that LOX-PP overexpression significantly reduced pAKT (S473; Figure 8B) compared with EV. NFκB, a downstream

effector of AKT, was also significantly reduced in LOX-PP overexpressed cells compared with EV (Figure 8C). BCL-2, an anti-apoptotic protein induced by NFκB, was also significantly decreased by the overexpression of LOX-PP in Y79 cells (Figure 8D). This was further confirmed by rLOX-PP-treated Y79 RB cells (Figure 9A), which show significantly decreased pAKT (S473; Figure 9B), NFκB (Figure 9C), and BCL-2 (Figure 9D). Additionally, the rLOX-PP exposed cells treated with wortmannin confirmed that the decreased expression of BCL2 was mediated through AKT signaling. Wortmannin treatment in rLOX-PP-exposed Y79 cells (Figure 10A) synergistically reduced the expression of AKT (Figure 10B), NFκB (Figure 10C), and BCL-2 (Figure 10D).
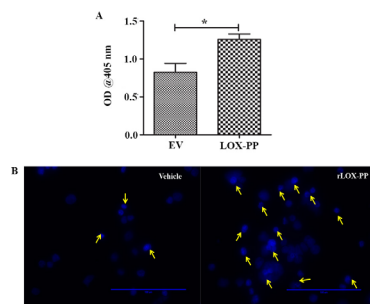

Figure 6. The role of LOX-PP in Y79 cell apoptosis. **A:** Quantification result of apoptosis by using the cell death ELISA kit. **B:** Microscopic image of apoptotic cells stained with DAPI upon treatment with rLOX-PP (yellow arrow shows apoptotic cells). Values were expressed as mean ± SD, n=3. (Student *t* test statistical analysis was used; ***p<0.001, **p<0.01, and *p<0.05*, when compared with EV) (EV, empty vector).
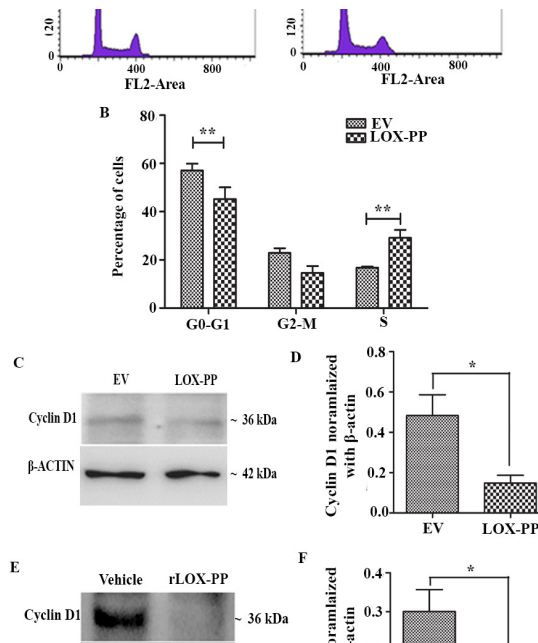
Figure 7. The role of LOX-PP in the cell cycle events in RB. **A:** Flow cytometric analysis and propidium iodide stain showing the percentage of cells in G2, S, and G1. **B:** Representative bar diagram of cell cycle analysis. **C:** Western blot analysis showing the expression of Cyclin D1 in Y79 cells were overexpressed with LOX-PP. **D:** The bar diagram represents the quantification of Cyclin D1 normalized with β-actin. **E:** Western blot for Cyclin D1 in Y79 cells upon treatment with 2.5µg/ml of rLOX-PP. **F:** The bar diagram shows the quantification of Cyclin D1. Values were expressed as mean ± SD, n=3. (Student *t* test statistical analysis was used; ***p<0.001,**p<0.01, and *p<0.05, when compared with EV and vehicle control) (EV, empty vector; RB, retinoblastoma).
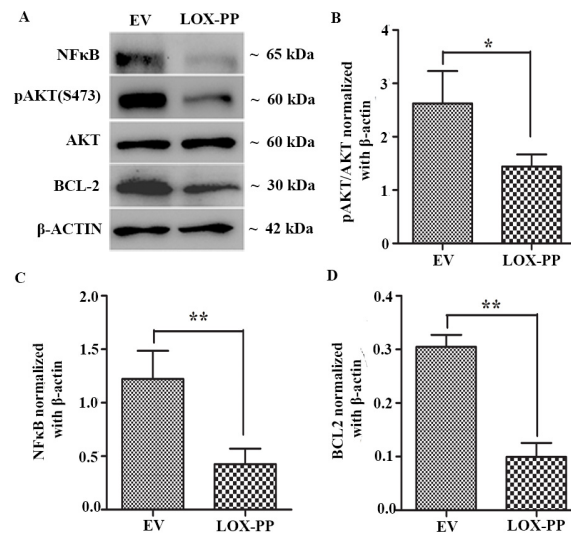

Figure 8. pAKT, NFκB, and BCL-2 protein expression upon LOX-PP overexpression. **A:** Y79 cells were overexpressed with LOX-PP, and whole-cell protein was extracted and subjected to western blot analysis for pAKT (S473), total AKT, NFκB, and BCL-2. **B:** The bar diagram shows the quantification of pAKT normalized with β-actin. **C:** The bar diagram shows the quantification of NFκB normalized with β-actin. **D:** The bar diagram shows the quantification of BCL-2 normalized with β-actin. Values were expressed as mean ± SD, n=3. (Student *t* test statistical analysis was used; ***p<0.001, **p<0.01, and *p<0.05, when compared with EV) (EV, empty vector).
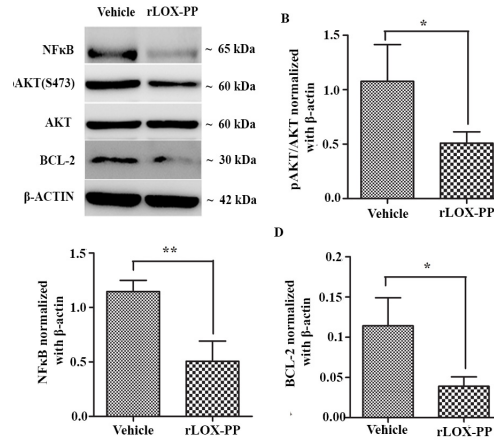
Figure 9. pAKT, NFκB, and BCL-2 protein expression on rLOX-PP addition. **A:** Western blot analysis showing the expression of pAKT (S473), AKT, NFκB, and BCL-2 in Y79 cells that were treated with 2.5 µg/ml of recombinant LOX-PP. **B:** The representative bar diagram shows the quantification of pAKT normalized with β-actin. **C:** The representative bar diagram shows the quantification of NFκB normalized with β-actin. **D:** The representative bar diagram shows the quantification of BCL-2 normalized with β-actin. Values were expressed as mean ± SD, n=3. (Student *t* test statistical analysis was used; ***p<0.001,**p<0.01, and *p<0.05, when compared with vehicle control)

DISCUSSION

Recent developments suggest that the primary modality for managing RB is chemo reduction, which can lower the incidence of enucleation and improve treatment outcomes. Marianna et al. have demonstrated that chemotherapeutic agents are capable of inducing apoptosis in cells engaged in active proliferation [28]. Tumor suppressors and proto-oncogenes are associated with proteins involved in proliferation and apoptosis [29]. LOX has a paradoxical role in tumor biology; the tumor-suppressor activity of LOX [30] has been delineated to its propeptide region through the inhibition of ras signaling in breast, pancreatic, prostate, and lung cancer [21,22,31-39]. Recently, Kosa et al. demonstrated that ras activation in a larger cluster of retinal progenitor cells induces tumor formation in the eye [40]. Bautista et al. and Cohen et al. reported that ras mutation in sporadic and heritable RB
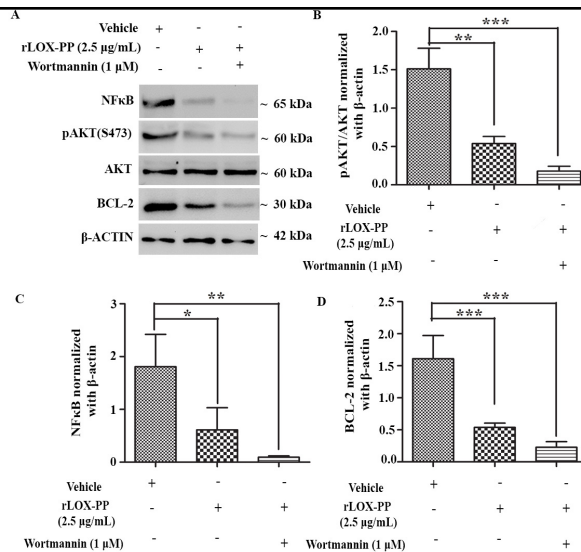

Figure 10. pAKT, NFκB, and BCL-2 protein expression on wortmannin-treated rLOX-PP exposed cells. **A:** Western blot analysis showing the expression of pAKT (S473), AKT, NFκB, and BCL-2 in Y79 cells were treated with 2.5 µg/ml of recombinant LOX-PP and 2.5 µg/ml of recombinant LOX-PP + 1 µM wortmannin. **B:** The representative bar diagram shows the quantification of pAKT normalized with β-actin. **C:** The representative bar diagram shows the quantification of NFκB normalized with β-actin. **D:** The representative bar diagram shows the quantification of BCL-2 normalized with β-actin. Values were expressed as mean ± SD, n=3. (One-way ANOVA statistical analysis was used; ***p<0.001, **p<0.01, and *p<0.05, when compared with vehicle control).

tumor tissue [41,42] with ras signaling dysregulated in RB [42]. A study by Yang et al. reveals the expression of LOX, although not observed in all RB tumor tissues and that upon hypoxia treatment, there is increased expression of LOX in Y79 and Weri RB1 cells [43]. In this study, we observed a lowered basal expression of LOX-PP in Y79 RB cells, and when LOX-PP was overexpressed, differential gene regulation was identified in pathways such as RB in cancer, apoptosis, cell cycle, FGFR2 signaling, and focal adhesion-PI3K-AKT. Here, we report for the first time the ability of LOX-PP to be pro-apoptotic in Y79 RB cells, thus playing a beneficial role. LOX-PP has been shown to sensitize breast cancer cells and pancreatic cells to doxorubicin treatment, thereby inducing apoptosis without injury of non-targeted tissue [44]. Bais et al. reported that rLOX-PP inhibits xenograft prostate cancer through the activation of the checkpoint kinase 2 and ataxia telangiectasia mutated (ATM) protein kinase, thereby increasing DNA fragmentation. rLOX-PP interacts with MRE11, which is a complex protein involved in the activation of ATM in response to DNA repair, and sensitizes the prostate cancer cells for ionizing radiation [37]. In concordance, our results show the deregulation of the DNA-repair mechanism pathway in LOX-PP-overexpressed Y79 RB cells. Chemotherapy-induced cytotoxicity has been reported to be less in P53 deficient animals compared to that of wild-type, suggesting the role of P53 in the protection of healthy cells [45]. We have found that overexpression of LOX-PP significantly reduces the transcript levels of *TP53* in Y79 RB cells.

Interestingly, *MDM2,* the regulator of *TP53*, was also increased by LOX-PP in Y79 RB cells. It is reported that MDM2 has become an important therapeutic target as it can act both as an oncogene and tumor suppressor gene. Functionally, MDM2 reduces the nuclear export of TP53, which is transcriptionally active, thereby enhancing cytoplasmic TP53 interaction with the BCL2 family of proteins leading to apoptosis [46]. Further, recent studies report that MDM2 controls cell cycle progression through controlling the RB overexpression [47]. Along similar lines, we found that LOX-PP reduced cell proliferation and increased apoptosis in Y79 cells.

The ras gene activates many distinct signal-transduction pathways, including RAF/MAPK/ERK and the PI3K/AKT pathway [48]. AKT, a serine/threonine-specific protein kinase being an essential mediator of ras signaling [34], plays a vital role in cellular processes such as apoptosis, cell proliferation, and cell migration [49]. NFκB, a downstream effector of AKT signaling, is a transcription factor involved in DNA transcription, cell proliferation, and apoptosis. The abnormal activation of NF-κB is reported in many primary cancers [50]. The anti-apoptotic gene, BCL-2, is an NF-κB target gene that is upregulated in pancreatic tumors [51]. siRNA targeting BCL-2 is reported as anti-proliferative and pro-apoptotic in pancreatic cancer cells [52]. Reports suggest inhibiting BCL-2 through repressing AKT-NFκB induces apoptosis in Y79 cells [49]. LOX-PP overexpression reduced BCL-2 mRNA and protein expression by lowering the p65 protein levels in PANC-1 and H1299 cells [34]. We also found that the overexpression of LOX-PP/exogenous addition of rLOX-PP reduced AKT activity and substantially reduced the activity of NFκB and thereby decreased BCL-2 protein expression, implicating increased apoptosis and decreased cell proliferation in Y79 cells. Moreover, LOX-PP overexpression arrested Y79 cells in S-phase, indicating the S-phase-mediated inhibition of cell proliferation by LOX-PP. Additionally, the decreased expression of the proliferation marker, PCNA [53], and Cyclin D1 in LOX-PP overexpressed/exogenously added rLOX-PP Y79 cells suggests the inhibition of proliferation. LOX-PP has been reported to have multiple cellular localizations in various cancer cells and interact with intracellular proteins [54]. In our previous publication, we showed that LOX-PP localized in the nucleus in endothelial cells [25]. In addition, Ozdener et al. found that rLOX-PP is primarily taken up through macropinocytosis in MDA-MB-231, PWR-1E, PC3, and SCC9 cell lines. The ionic strength of highly basic rLOX-PP prevents endosomal acidification thereby entering into the cytoplasm, interacting with intracellular targets, and executing its function [55]. Therefore, we speculate that rLOX-PP can exert its function intracellularly although we have not demonstrated it in this cell. To summarize, these results suggest the therapeutic potential of LOX-PP in RB. The limitations of the current study are that we have not quantified the expression of LOX-PP in a RB tumor tissue and the functional assays have been performed in only Y79 RB cell lines. In conclusion, our data highlights the fact that LOX-PP overexpression/addition in human Y79 RB cells increases apoptosis and decreases cell proliferation through the repression of AKT-NFκB axis, thereby reducing BCL-2 protein expression in vitro. Organoid models, which mirror in vivo conditions, can be used to further establish the anti-tumorigenic activity of LOX-PP. This would add impetus to explore the therapeutic potential of LOX-PP in RB.

APPENDIX 1. STR ANALYSIS.

To access the data, click or select the words "Appendix 1."

APPENDIX 2. SUPPLEMENTARY FIGURE 1.

To access the data, click or select the words "Appendix 2."

APPENDIX 3. SUPPLEMENTARY FIGURE 2.

To access the data, click or select the words "Appendix 3."

REFERENCES

1. Jain M, Rojanaporn D, Chawla B, Sundar G, Gopal L, Khetan V. Retinoblastoma in Asia. Eye (Lond) 2019; 33:87-96[PMID: 30385881].

2. Knudson AG. Mutation and Cancer: Statistical Study of Retinoblastoma. Proc Natl Acad Sci USA 1971; 68:820-3. [PMID: 5279523].

3. Li P, Li Z. Effects of NF-κB and hypoxia on the biological behavior of Y79 retinoblastoma cells. Int J Clin Exp Pathol 2015; 8:1725-30. [PMID: 25973060].

4. Xu XL, Singh HP, Wang L, Qi DL, Poulos BK, Abramson DH, Jhanwar SC, Cobrinik D. Rb suppresses human cone-precursor-derived retinoblastoma tumours. Nature 2014; 514:385-8. Internet[PMID: 25252974].

5. Lohmann DR, Gallie BL. Retinoblastoma: Revisiting the model prototype of inherited cancer. Am J Med Genet 2004; 129C:23-8. [PMID: 15264269].

6. Models N, Che P, Louie K, Marcus KT, Holcombe VN, Schafer P, Aguilar-cordova CE. Metastatic and nonmetastatic models of retinoblastomaRetinoblastoma. 2000; 157:1405-12. .

7. Webb AH, Gao BT, Goldsmith ZK, Irvine AS, Saleh N, Lee RP, Lendermon JB, Bheemreddy R, Zhang Q, Brennan RC, Johnson D, Steinle JJ, Wilson MW, Morales-Tirado VM. Inhibition of MMP-2 and MMP-9 decreases cellular migration, and angiogenesis in in vitro models of retinoblastoma. BMC Cancer 2017; 17:434-[PMID: 28633655].

8. Apte RS, Harbour JW. Inhibiting Angiogenesis in Retinoblastoma. Ophthalmic Res 2007; 39:188-90. [PMID: 17556838].

9. Eng C, Li FP, Abramson DH, Ellsworth RM, Wong FL, Goldman MB, Seddon J, Tarbell N, Boice JD. Mortality From Second Tumors Among Long-Term Survivors of Retinoblastoma. JNCI J Natl Cancer Inst. 1993; 85:1121-8. [PMID: 8320741].

10. Liu H, Zhang Y, Zhang YY, Li YP, Hua ZQ, Zhang CJ, Wu KC, Yu F, Zhang Y, Su J, Jin ZB. Human embryonic stem cell-derived organoid retinoblastoma reveals a cancerous origin. Proc Natl Acad Sci USA 2020; 117:33628-38. [PMID: 33318192].

11. Li Y-P, Wang Y-T, Wang W, Zhang X, Shen R-J, Jin K, Jin L-W, Jin Z-B. Second hit impels oncogenesis of retinoblastoma in patient-induced pluripotent stem cell-derived retinal organoids: direct evidence for Knudson's theory. PNAS Nexus. 2022; 1:1-13. [PMID: 36714839].

12. Kagan HM, Trackman PC. Properties and function of lysyl oxidase. Am J Respir Cell Mol Biol 1991; 5:206-10. [PMID: 1680355].

13. Kagan HM, Li W. Lysyl oxidase: properties, specificity, and biological roles inside and outside of the cell. J Cell Biochem 2003; 88:660-72. [PMID: 12577300].

14. Bedell-Hogan D, Trackman P, Abrams W, Rosenbloom J, Kagan H. Oxidation, cross-linking, and insolubilization of recombinant tropoelastin by purified lysyl oxidase. J Biol Chem 1993; 268:10345-50. [PMID: 8098038].

15. Panchenko MV, Stetler-Stevenson WG, Trubetskoy OV, Gacheru SN, Kagan HM. Metalloproteinase activity secreted by fibrogenic cells in the processing of prolysyl oxidase. Potential role of procollagen C-proteinase. J Biol Chem 1996; 271:7113-9. [PMID: 8636146].

16. Trackman PC, Bedell-Hogan D, Tang J, Kagan HM. Post-translational glycosylation and proteolytic processing of a lysyl oxidase precursor. J Biol Chem 1992; 67:8666-71. [PMID: 1349020].

17. Uzel MI, Scott IC, Babakhanlou-Chase H, Palamakumbura AH, Pappano WN, Hong HH, Greenspan DS, Trackman PC. Multiple bone morphogenetic protein 1-related mammalian metalloproteinases process pro-lysyl oxidase at the correct physiological site and control lysyl oxidase activation in mouse embryo fibroblast cultures. J Biol Chem 2001; 276:22537-43. [PMID: 11313359].

18. Contente S, Kenyon K, Rimoldi D, Friedman RM, Kagan H, Friedman R. Expression of gene rrg is associated with reversion of NIH 3T3 transformed by LTR-c-H-ras. Science 1990; 249:796-8. [PMID: 1697103].

19. Kenyon K, Contente S, Trackman PC, Tang J, Kagan HM, Friedman RM. Lysyl oxidase and rrg messenger RNA. Science 1991; 253:802-[PMID: 1678898].

20. Kuivaniemi H, Korhonen RM, Vaheri A, Kivirikko KI. Deficient production of lysyl oxidase in cultures of malignantly transformed human cells. FEBS Lett 1986; 195:261-4. [PMID: 3753686].

21. Palamakumbura AH, Jeay S, Guo Y, Pischon N, Sommer P, Sonenshein GE, Trackman PC. The propeptide domain of

lysyl oxidase induces phenotypic reversion of ras-transformed cells. J Biol Chem 2004; 279:40593-600. [PMID: 15277520].

22. Min C, Kirsch KH, Zhao Y, Jeay S, Palamakumbura AH, Trackman PC, Sonenshein GE. The tumor suppressor activity of the lysyl oxidase propeptide reverses the invasive phenotype of Her-2/neu-driven breast cancer. Cancer Res 2007; 67:1105-12. [PMID: 17283144].

23. Srinivasan V. Palanisamy Karthikka KC, Subbulakshmi Chidambaram PR and, Natarajan SK. Expression and localisation of adiponectin and Its receptors in human ocular tissues. Int J Pharma Bio Sci 2014; 5:639-46. .

24. Livak KJ, Schmittgen TD. Analysis of relative gene expression data using real-time quantitative PCR and the 2(-Delta Delta C(T)) Method. Methods. 2001; 25:402-8. [PMID: 11846609].

25. Nareshkumar RN, Sulochana KN, Coral K. Inhibition of angiogenesis in endothelial cells by Human Lysyl oxidase propeptide. Sci Rep 2018; 8:10426-[PMID: 29993014].

26. Zeng Z, Gao ZL, Zhang ZP, Jiang HB, Yang CQ, Yang J, Xia XB. Downregulation of CKS1B restrains the proliferation, migration, invasion and angiogenesis of retinoblastoma cells through the MEK/ERK signaling pathway. Int J Mol Med 2019; 44:103-14. [PMID: 31115482].

27. Giuliano M, Lauricella M, Calvaruso G, Carabillò M, Emanuele S, Vento R, Tesoriere G. The apoptotic effects and synergistic interaction of sodium butyrate and MG132 in human retinoblastoma Y79 cells. Cancer Res 1999; 59:5586-95. [PMID: 10554039].

28. Lauricella M, Giuliano M, Emanuele S, Vento R, Tesoriere G. Apoptotic effects of different drugs on cultured retinoblastoma Y79 cells. Tumour Biol 1998; 19:356-63. [PMID: 9701726].

29. Zhou Q-M, Wang X-F, Liu X-J, Zhang H, Lu Y-Y, Huang S, Su S-B. Curcumin improves MMC-based chemotherapy by simultaneously sensitising cancer cells to MMC and reducing MMC-associated side-effects. Eur J Cancer 2011; 47:2240-7. [PMID: 21616659].

30. Payne SL, Hendrix MJC, Kirschmann DA. Paradoxical roles for lysyl oxidases in cancer–a prospect. J Cell Biochem 2007; 101:1338-54. [PMID: 17471532].

31. Sánchez-Morgan N, Kirsch KH, Trackman PC, Sonenshein GE. UXT Is a LOX-PP Interacting Protein That Modulates Estrogen Receptor Alpha Activity in Breast Cancer Cells. J Cell Biochem 2017; 118:2347-56. [PMID: 28106301].

32. Palamakumbura AH, Vora SR, Nugent MA, Kirsch KH, Sonenshein GE, Trackman PC. Lysyl oxidase propeptide inhibits prostate cancer cell growth by mechanisms that target FGF-2-cell binding and signaling. Oncogene 2009; 28:3390-400. [PMID: 19597471].

33. Min C, Zhao Y, Romagnoli M, Trackman PC, Sonenshein GE, Kirsch KH. Lysyl oxidase propeptide sensitizes pancreatic and breast cells to doxorubicin-induced apoptosis. J Cell Biochem 2010; 111:1160-8. [PMID: 20717927].

34. Wu M, Min C, Wang X, Yu Z, Kirsch KH, Trackman PC, Sonenshein GE. Repression of BCL2 by the tumor suppressor activity of the lysyl oxidase propeptide inhibits transformed phenotype of lung and pancreatic cancer cells. Cancer Res 2007; 67:6278-85. [PMID: 17616686].

35. Zhao Y, Min C, Vora SR, Trackman PC, Sonenshein GE, Kirsch KH. The lysyl oxidase pro-peptide attenuates fibronectin-mediated activation of focal adhesion kinase and p130Cas in breast cancer cells. J Biol Chem 2009; 284:1385-93. [PMID: 19029090].

36. Min C, Yu Z, Kirsch KH, Zhao Y, Vora SR, Trackman PC, Spicer DB, Rosenberg L, Palmer JR, Sonenshein GE. A loss-of-function polymorphism in the propeptide domain of the LOX gene and breast cancer. Cancer Res 2009; 69:6685-93. [PMID: 19654310].

37. Bais MV, Ozdener GB, Sonenshein GE, Trackman PC. Effects of tumor-suppressor lysyl oxidase propeptide on prostate cancer xenograft growth and its direct interactions with DNA repair pathways. Oncogene 2015; 34:1928-37. [PMID: 24882580].

38. Sato S, Trackman PC, Mäki JM, Myllyharju J, Kirsch KH, Sonenshein GE. The Ras signaling inhibitor LOX-PP interacts with Hsp70 and c-Raf to reduce Erk activation and transformed phenotype of breast cancer cells. Mol Cell Biol 2011; 31:2683-95. [PMID: 21536655].

39. Sánchez-Morgan N, Kirsch KH, Trackman PC, Sonenshein GE. The lysyl oxidase propeptide interacts with the receptor-type protein tyrosine phosphatase kappa and inhibits β-catenin transcriptional activity in lung cancer cells. Mol Cell Biol 2011; 31:3286-97. [PMID: 21690299].

40. Koso H, Tsuhako A, Matsubara D, Fujita Y, Watanabe S. Ras activation in retinal progenitor cells induces tumor formation in the eye. Exp Eye Res 2019; 180:39-42. [PMID: 30500365].

41. Bautista D, Emanuel JR, Granville C, Howard R, Costa J. Identification of mutations in the Ki-ras gene in human retinoblastoma. Invest Ophthalmol Vis Sci 1996; 37:2313-7. [PMID: 8843915].

42. Cohen Y, Merhavi-Shoham E, Avraham-Lubin BCR, Savetsky M, Frenkel S, Pe'er J, Goldenberg-Cohen N. PI3K/Akt Pathway Mutations in Retinoblastoma. Invest Opthalmol Vis Sci. 2009; 50:5054-[PMID: 19420344].

43. Yang Q, Tripathy A, Yu W, Eberhart CG, Asnaghi L. Hypoxia inhibits growth, proliferation, and increases response to chemotherapy in retinoblastoma cells. Exp Eye Res 2017; 162:48-61. [PMID: 28689747].

44. Min C, Zhao Y, Romagnoli M, Trackman PC, Sonenshein GE, Kirsch KH. Lysyl oxidase propeptide sensitizes pancreatic and breast cells to doxorubicin-induced apoptosis. J Cell Biochem 2010; 111:1160-8. [PMID: 20717927].

45. Gudkov AV, Komarova EA. Dangerous habits of a security guard: the two faces of p53 as a drug target. Hum Mol Genet 2007; 16:R67-72. [PMID: 17613549].

46. Manfredi JJ. The Mdm2-p53 relationship evolves: Mdm2 swings both ways as an oncogene and a tumor suppressor. Genes Dev 2010; 24:1580-9. [PMID: 20679392].

47. Hernandez-Monge J, Martínez-Sánchez M, Rousset-Roman A, Medina-Medina I, Olivares-Illana V. MDM2 regulates RB levels during genotoxic stress. EMBO Rep 2021; 22:e50615[PMID: 33185004].

48. Arsura M, Mercurio F, Oliver AL, Thorgeirsson SS, Sonenshein GE. Role of the IkappaB kinase complex in oncogenic Ras- and Raf-mediated transformation of rat liver epithelial cells. Mol Cell Biol 2000; 20:5381-91. [PMID: 10891479].

49. Zheng Q, Zhang Y, Ren Y, Wu Y, Yang S, Zhang Y, Chen H, Li W, Zhu Y. Antiproliferative and apoptotic effects of indomethacin on human retinoblastoma cell line Y79 and the involvement of β-catenin, nuclear factor-κB and Akt signaling pathways. Ophthalmic Res 2014; 51:109-15. [PMID: 24355977].

50. Rayet B, Gélinas C. Aberrant rel/nfkb genes and activity in human cancer. Oncogene 1999; 18:6938-47. [PMID: 10602468].

51. Fujioka S, Sclabas GM, Schmidt C, Frederick WA, Dong QG, Abbruzzese JL, Evans DB, Baker C, Chiao PJ. Function of nuclear factor kappaB in pancreatic cancer metastasis. Clin Cancer Res 2003; 9:346-54. [PMID: 12538487].

52. Ocker M, Neureiter D, Lueders M, Zopf S, Ganslmayer M, Hahn EG, Herold C, Schuppan D. Variants of bcl-2 specific siRNA for silencing antiapoptotic bcl-2 in pancreatic cancer. Gut 2005; 54:1298-308. [PMID: 16099798].

53. Kamei S, Sakayama K, Tamashiro S, Aizawa J, Miyawaki J, Miyazaki T, Yamamoto H, Norimatsu Y, Masuno H. Ketoprofen in topical formulation decreases the matrix metalloproteinase-2 expression and pulmonary metastatic incidence in nude mice with osteosarcoma. J Orthop Res 2009; 27:909-15. [PMID: 19105229].

54. Sanchez-Morgan N, Kirsch KH, Trackman PC, Sonenshein GE. The Lysyl Oxidase Propeptide Interacts with the Receptor-Type Protein Tyrosine Phosphatase Kappa and Inhibits -Catenin Transcriptional Activity in Lung Cancer Cells. Mol Cell Biol 2011; 31:3286-97. [PMID: 21690299].

55. Ozdener GB, Bais MV, Trackman PC. Determination of cell uptake pathways for tumor inhibitor lysyl oxidase propeptide. Mol Oncol 2016; 10:1-23. [PMID: 26297052].